Central European Geology, Vol. 60/1, 53–72 (2017)
DOI: 10.1556/24.59.2016.005
First published online December 21, 2016

Ore geology of the copper sulfide mineralization in the Rudabánya ore-bearing complex

Norbert Németh*, János Földessy, Judit Turi

Institute of Mineralogy and Geology, Faculty of Earth Science and Engineering, University of Miskolc, Miskolc, Hungary

Received: July 18, 2016; accepted: September 21, 2016

The mineralized complex of Rudabánya hosts deposits of several mineral resources including base metal ores. Recent exploration provided new information on the enrichment of copper within this complex. The primary copper mineralization consists of sulfides. The paragenetic sequence starts with fahlore, continues with bornite, and concludes in chalcopyrite formation partly replacing the former phases. It is hosted by brecciated carbonate rocks, overprinting the paragenesis of the iron metasomatism. It was found to be spatially separated from zinc and lead enrichments. Oxidation and a subsequent new pulse of mineralization formed several new copper, zinc, and lead minerals, probably by the remobilization of the primary parageneses.

Keywords: base metal ore, bornite, chalcopyrite, fahlore, North Hungary, sediment hosted ore

Introduction

Rudabánya is a historic mining town in NE Hungary. Documented medieval mining activities were targeted on copper and silver ore cropping out in a hill range extending northeastward of the town. Beginning with the 19th century, iron ores attracted the mining entrepreneurs. Limonite, later also siderite ore, was exploited both with opencast and underground mining. Until the suspension of ore mining in 1985, more than 4 km long and 1.5 km wide area was transformed into a series of open pits

*Corresponding author: Norbert Németh; Institute of Mineralogy and Geology, Faculty of Earth Science and Engineering, University of Miskolc, H-3515 Miskolc-Egyetemváros, Hungary
E-mail: foldnn@uni-miskolc.hu

ISSN 1788-2281

and waste dumps. Historic exploration activity with approximately 2,800 boreholes also extended to the few kilometer broader vicinity of this area. The history of mining, exploration, and geology of the ore-bearing complex was documented in detail by Pantó et al. (1957) and Balla (1987).

This area hosts a complex assemblage of different ore deposits with an equally complex mineralogy and a strong tectonic overprint. Beyond the traditionally mined iron ores (and as byproduct, copper), zinc, lead, mercury, precious metals, barite, gypsum, and lignite resources also had an economic impact. Prospecting interest did not cease with the suspension of mining. A geochemical exploration project in the 1990s studied the possibility of a Carlin-type mineralization (Korpás et al. 1999). Despite the long exploration history, genetic problems and relationships of the ore deposits are far from being solved.

A recent base metal ore exploration project, begun in 2007 with the participation of the Institute of Mineralogy and Geology, University of Miskolc, provided us with a framework for revising the ore geological model established in the 1950s (Pantó 1956), subsequently refined by a variety of mineralogical and geological evidences summarized by Szakáll (2001). Approximately, 260 assays were obtained from channel samples of pit walls, exploration trenches (750 m altogether), and tunnels. Nineteen vertical or oblique holes (2,544 m altogether) were cored, and 925 assays were obtained from core samples. Beyond these, surface mapping and sampling (also including waste dumps and soil geochemical survey outside the pits) provided further observations. Several results of this exploration activity were published (Földessy et al. 2010, 2012a, 2012b, 2014; Kristály et al. 2010; Bodor et al. 2013a, 2013b; Németh et al. 2013; Németh and Kasó 2014). This paper does not attempt to give a complex overview of all these studies; it is devoted primarily to the topic of the primary copper sulfide mineralization, the study of which also yielded new results, modifying the previous model.

Ore geological and mineralogical outlines of the Rudabánya ore-bearing complex

The rocks of the Rudabánya ore-bearing complex belong to the Silicikum stratigraphic superunit (Kovács et al. 1989; Szentpétery and Less 2006), which is widely distributed N of Rudabánya in the Silica Nappe. This succession begins with sediments of a Permian–Early Triassic transgression and is characterized by the evolution of carbonate platforms and basins during the Middle and Late Triassic. The deposits are hosted by tectonically disturbed and metasomatized sedimentary rocks, situated in the Darnó Zone, an approximately 100 km long, NNE–SSW striking regional strike-slip fault zone with variable activity during the Cenozoic (Zelenka et al. 1983; Fodor et al. 1999). The zone also contains low-grade metamorphic rocks, Jurassic mélange, and serpentinized ophiolite bodies derived from tectonic units other than the Silica Nappe. Approximately 65 km SSW of Rudabánya, along this

zone occurs the significant porphyry and skarn copper ore deposit of Recsk. However, there is no evidence of any magmatism affecting the ore-forming processes at Rudabánya.

The Lower Triassic succession of the Silicikum begins with carbonate-cemented pelitic and psammitic siliciclastic rocks consisting mainly of quartz fragments (Bódvaszilas Sandstone Fm.); thereafter, the carbonate content gradually increases in the pelitic formations (Szin Marl Fm. and Szinpetri Limestone Fm.) to an overlying, thick-bedded or massive dolomite and limestone of anoxic facies (Gutenstein Fm.; Szentpétery and Less 2006). This succession can be identified in the mineralized complex cropping out in the mining area NNE of Rudabánya, situated in approximately 1.5 km wide zone bordered by master faults of the Darnó Zone, uplifted from the Neogene sediment-covered environment. The rocks in this regional fault zone are fragmented, brecciated, and have an imbricate and blocky structure; 10–100 m scale carbonate blocks are embedded in a fine-grained, marly matrix.

These blocks, originating mostly from the dolomite of the Gutenstein Fm., were subjected to siderite-forming metasomatism in the core of the zone and partly altered at the edges (Pantó 1956). This formation is the primary siderite iron ore, and was also the protolith of the secondary limonite ore. Original (now mostly extracted) outcropping bodies were limonitized together with their country rocks, containing a rich and spectacular secondary assemblage of base metal minerals. These metals occur in the form of sulfides in the siderite bodies along with barite. Ankerite nodes and cement can also be found in the underlying sandstone and siltstone (Bodor et al. 2013a, 2013b). The occurrence of barite, pyrite, and further sulfide minerals is also typical for these nodes, while the bulk of the siliciclastic rocks (except for the limonitized parts) is barren. The overlying sedimentary succession starts with the Upper Oligocene at the boundaries and with the Pannonian stage in the central zone; these sediments are not affected by any base metal mineralization. The unconformity shows the existence of a long Neogene and also a pre-Neogene period of weathering.

Galena and accessory sphalerite were known minerals of the siderite deposit in the barite-enriched edge zone of the ore blocks ("baritic spar edge"; Pantó 1956). In some cases, the lead mineralization of that type consists of alternating barite and sulfide-rich stripes; more frequently, it shows a brecciated structure with cm-scale carbonate, barite, and sulfide nodes of large grain size, and also cm-scale clasts. In other cases, ore minerals occur in the clasts of a breccia; thus, the evolved ore was subsequently fragmented. Galena lenses can also be found in the marly country rock of the carbonate blocks, regarded as clasts previously sheared from the edges of the blocks. In an earlier phase of our exploration, it was observed that in some cases this material occurs in folded layers, and evidence was interpreted to define a new stratiform zinc–lead ore deposit type hosted by the underlying marl (Földessy et al. 2010; Németh et al. 2013). This ore (and the carbonate-bound type as well) also contains sphalerite beyond galena, and Zn content exceeds Pb by a factor of 4–5.

The sphalerite, however, is hard to recognize because of the minute (<0.1 mm) grain size and pale color.

Copper ore at Rudabánya

The copper content of the Rudabánya iron ore is a well-known feature since early times. Pantó (1956) estimated 0.15 wt% as the average Cu content of the primary siderite iron ore, mainly in the form of chalcopyrite with accessory bornite and tetrahedrite, unevenly enriched in the "spar edge." Koch et al. (1950) also described chalcopyrite (which substitutes siderite, pyrite, and barite as well) as the main primary copper-bearing mineral phase. The model established by these studies interpreted the development of siderite, barite, and base metal sulfides in a continuous paragenetic sequence.

Pantó (1956) and fellow geologists considered base metal minerals as deleterious accessories of the iron ore, which cause problems for processing, and not as ores of considerable economic value. From the 1970s (until 1982), the geologists began to pay attention to other potential mining products than iron ore, and copper ores were also exploited and sold. Documentations of newer boreholes of the "Rb" series contain regular observations of barite, chalcopyrite, and galena content, and assays of Cu and Pb content of the rocks. Between 1976 and 1985, 120 boreholes were completed and aimed at defining base metal resources. The Hungarian Geological Institute made a geochemical survey (Csalagovits 1973), from some hundreds of samples from the pit walls and the drill cores. They found enrichments of silver, copper, manganese, lead, and zinc in carbonates as well as in siliciclastic rocks, but with peak concentrations in barite-containing edge zones of the siderite ore bodies. Minor enrichment was also indicated in the Middle–Upper Triassic rocks.

Records of copper ore reserves since 1971 and of lead ore reserves since 1972 were kept by the Hungarian Ore and Mineral Mining Co. A manuscript of the 1982 resource estimation has been localized in the archive. The total of the estimated, indicated, and inferred Cu ore resource according to this document is 1,548 kt, with the following grades: Cu 0.56% and Fe 18.93%. The copper ores were not assayed for Pb or Zn, and only two blocks have Ag data (<10 ppm).

The company started Induced polarization (IP) measurements over galena indications known from boreholes (Balla 1987). In the 1960s, IP measurements were made to gain experience in using it to determine the sulfide content with a fairly good result for pyrite enrichment underground and in well logs, but less successfully at surface. At IP surveys extended to the marginal zone, the effect of sulfides was surpassed by the effect of graphitic shale (Szalay et al. 1974).

Mineralogical studies were carried out with modern methods, and increasing evidence improved the deposit model. According to the description of Szakáll (2001), copper sulfides occur with sparry carbonate crystals (sometimes at cm-scale) in nodes and veins within a country rock comprising zoned, sideritized carbonates. It

was observed and recorded that Cu and Pb–Zn sulfides occur separately, which may suggest different genetic conditions. It also became clear, as supported by the measurements for the estimation of crystallization temperatures (Nagy 1982; Pósfai 1989), that barite and sulfides may have been formed in more than one phase. A late and relatively low-temperature hydrothermal mineralization was recognized, which also affected limonitized ore bodies.

Samples and analytical methods

The sampling was carried out on open pit walls, exploration trenches, and cores from exploration boreholes (Fig. 1). Typical sampling interval of both the channels

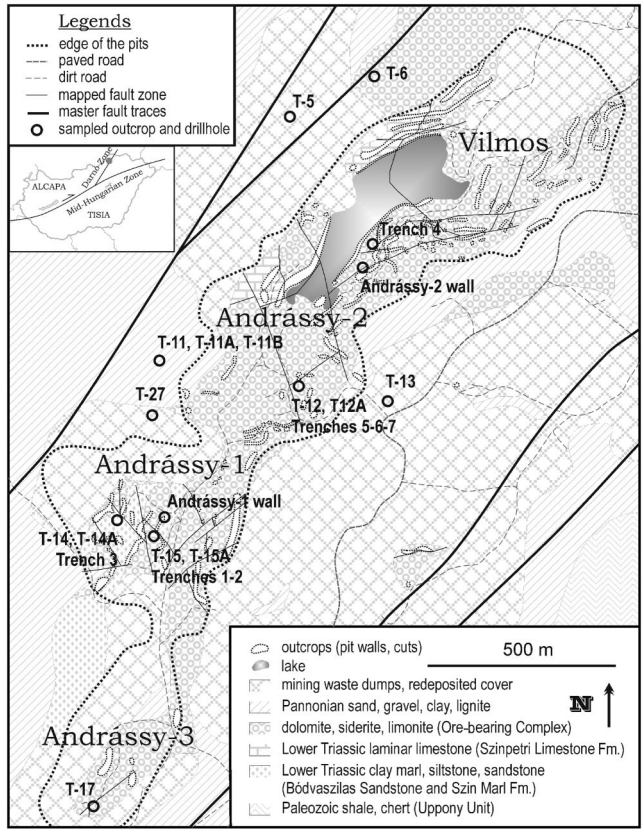

Fig. 1
Sketch map of the Rudabánya mining area with the location of new exploration boreholes and other sampling sites. Insert shows the position of Rudabánya within Hungary

and the half-cut cores was 1 m. Assays were made for 35 elements with Inductively Coupled Plasma Optical Emission Spectrometry (ICP-OES; after aqua regia digestion) and Inductively Coupled Plasma Atomic Emission Spectroscopy (ICP-AES) for gold by the ALS Global laboratory. As the primary targets were the host bodies of base metal sulfide mineralization, sampling was concentrated on sites and core sections with visible sulfide enrichment and, if possible, assayed copper enrichment, avoiding the limonitized bodies. Even so, scarcely any samples are free from oxidation features. The zinc–lead ores and copper ores occur definitely separated in the collected material, so observations regarding these can be separated as well, and the description of the next chapters characterizes the copper ores.

Ore microscopy (Fig. 2) was done using a Zeiss Axioplan polarization microscope in the Institute of Mineralogy and Geology, University of Miskolc; the observations of Kupi (2011) at the laboratory of the University of Oviedo were also used. Back-scattered electron images (Fig. 3) and microprobe assays were carried out on polished sample surfaces with the JEOL JXA-8600 Superprobe in the Institute of Mineralogy and Geology, University of Miskolc, in EDAX type energy dispersive system without standards, at 20 kV accelerating voltage and 20 nA probe current. The compositional data obtained by this method cannot be regarded as exact values, but the incorporation of certain elements into the minerals is indicated by measured numbers.

Results from borehole assays

During the recent exploration campaign, numerous boreholes intersected the copper ore mineralization at shallow depth. One of these, the T-12 borehole (Fig. 1), was selected for illustration. Its simplified lithological log and chemical composition are shown in Table 1. The assays were generally at 1.0 m length half-core samples. In the table, composite values of mineralized intervals (using >0.2% Cu and >0.5% Pb and Zn, min. 2.0 m length cut-off) are shown.

The borehole log shows the following highlighted features:

- High Cu values and high Pb and Zn values are adjacent but separated, and lithologically controlled (Cu is hosted predominantly in dolomite, Pb and Zn in shale and siltstone). The oxidation zone includes a mixed geochemical assemblage with Fe, Cu, Pb, and Zn enrichments.
- The T-12 borehole assay results show that the base metal mineralization is not necessarily linked to margins of siderite bodies since Cu, Pb, and Zn values are anomalous without significant parallel iron enrichment.
- Underlying sandstone is characterized by typically low base metal concentrations. Assays obtained from carbonate bodies and from their carbonate-cemented siltstone matrix are generally significantly higher.
- Copper mineralization is related to one specific lithology, namely, the dolomite breccia. Once lithology changes (e.g., to siltstone breccia), copper mineralization diminishes.

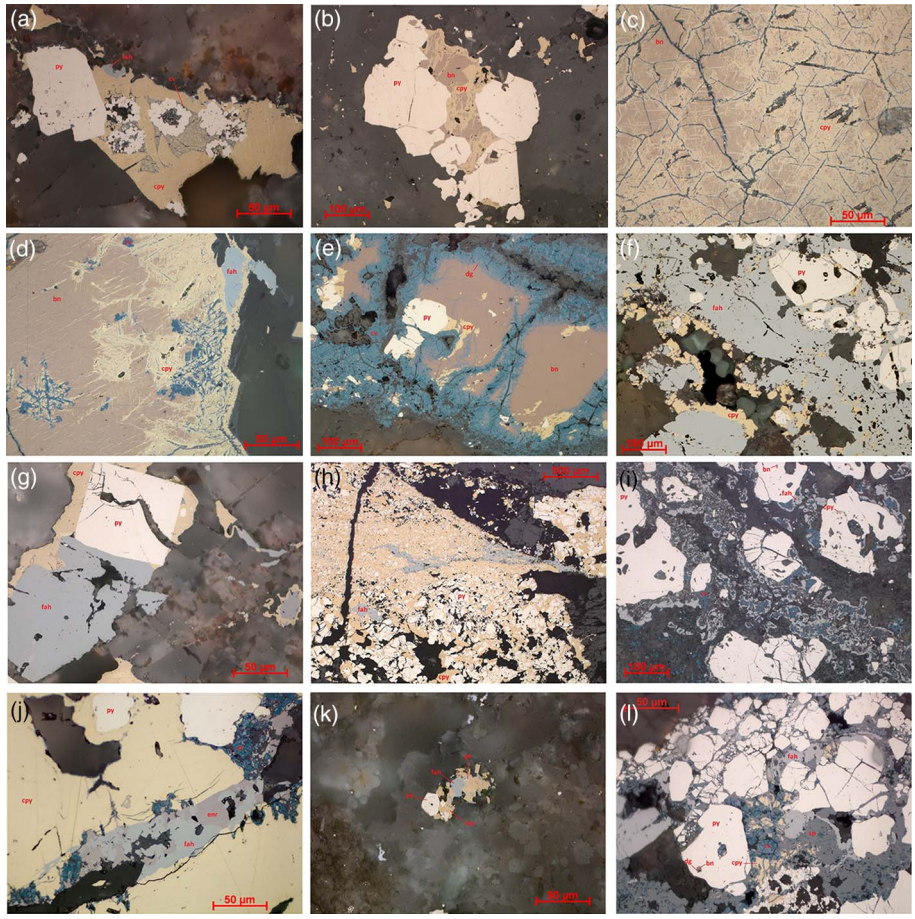

Fig. 2
Microscopic images of sections from the samples. Sites are shown in Fig. 1. (a) Chalcopyrite partly altered to covellite overgrown on concentric pyrite assemblages (Trench 2). (b) Pyrite overgrown by bornite, partly substituted by chalcopyrite (T-12; 38.1 m). (c and d) Characteristic lamellar substitution of bornite by chalcopyrite, with chalcopyrite partly altered to covellite in the second case (Andrássy-2 wall). (e) Bornite altered to digenite at the grain edges and chalcopyrite substituting bornite, mostly altered to covellite (wall at Trench 5). (f) Chalcopyrite substituting fahlore (grown on pyrite) along fractures and grain edges (wall at Trench 1). (g) Pyrite and fahlore overgrown by chalcopyrite (wall at Trench 1). (h) Fahlore of the second group in fractures of chalcopyrite grown on pyrite (Andrássy-2 wall). (i) Pyrite with bornite inclusion overgrown by fahlore partly altered to covellite (Trench 3). (j) Fahlore of the second (and also third) group and enargite (probably also famatinite) as vein filling in chalcopyrite (Andrássy-1 wall). (k) Galena and pyrite overgrown by tetrahedrite, substituted subsequently by chalcopyrite (T-5; 137.4 m). (l) Chalcopyrite altered to covellite, overgrown by fahlore of the second group and sphalerite (wall at Trench 3). Abbreviations: bn – bornite, cpy – chalcopyrite, cv – covellite, dg – digenite, enr – enargite, fah – fahlore, gn – galena, py – pyrite, and sp – sphalerite

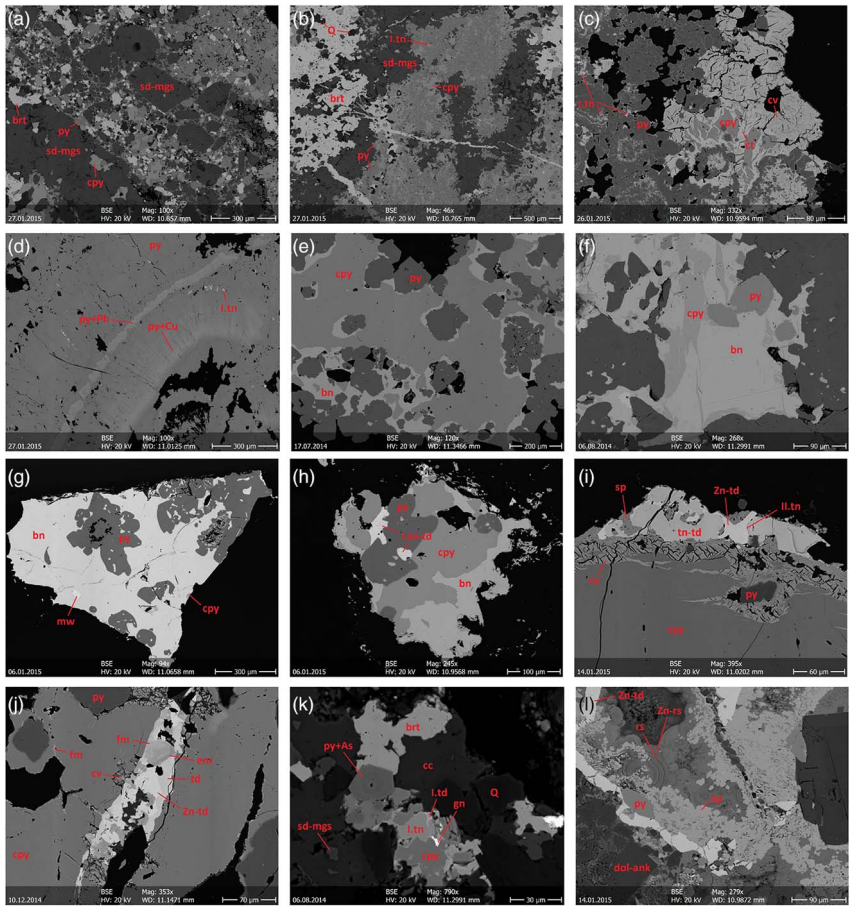

Fig. 3
Backscattered electrons (BSE) images of the studied samples. Sites are shown in Fig. 1. (a) Pyrite, barite, and chalcopyrite in the matrix of carbonate breccia of siderite–magnesite composition (T-27; 78.8 m). (b) Pyrite, tennantite, and chalcopyrite overgrown on carbonate clasts of siderite–magnesite composition; barite with quartz and in veins crosscutting the sulfide assemblage (T-27: 78.8 m). (c) Zoned intergrowth of tennantite and pyrite; next to it, chalcopyrite altered to covellite and chalcocite (Andrássy-1 wall). (d) Pyrite assemblage with zoned copper and lead enrichment (T-27; 50.9 m). (e) Hypidiomorph pyrite and carbonates overgrown by bornite and void filling chalcopyrite (T-12; 38.1 m). (f) Flame structure of chalcopyrite within bornite (T-5; 154.1 m). (g) Bornite with mawsonite and chalcopyrite, overgrown on concentric pyrite assemblages (T-12; 162.7 m). (h) Fahlore grains of the first group as inclusions in pyrite, bornite, and chalcopyrite (T-12; 162 m). (i) Fahlore of the second and third groups and sphalerite growing on chalcopyrite edge altered to covellite (wall at Trench 3). (j) Vein in chalcopyrite: tetrahedrite, Zn-tetrahedrite, enargite, and famatinite (Andrássy-1 wall). (k) Galena and As-containing pyrite overgrown by fahlore and chalcopyrite (T-5; 137.4 m). (l) Zn-tetrahedrite, Zn-zoned rosasite, and sphalerite in the matrix of carbonate breccia of dolomite–ankerite composition (wall at Trench 3). Abbreviations: bn – bornite, brt – barite, cpy – chalcopyrite, cv – covellite, ct – chalcocite, dg – digenite, enr – enargite, fm – famatinite, gn – galena, mw – mawsonite, py – pyrite, Q – quartz, rs – rosasite, sd-mgs – carbonate of siderite–magnesite composition, sp – sphalerite, td – tetrahedrite, and tn – tennantite

Table 1
Simplified lithological and assay log of the T-12 drillhole. Concentration values are weighted averages of the assayed samples from the indicated interval; waste dump was not assayed. Cu and Zn–Pb enriched intervals are highlighted with bold and italic numbers, respectively

Start depth	End depth	Age		Rock type	Ag (ppm)	Ba (ppm)	Cu (ppm)	Fe (%)	Pb (ppm)	S (%)	Zn (ppm)
0.00	6.50	Recent		Waste dump material							
6.50	18.30	Anisian	Zone of oxidation	Dolomite	**5**	**71**	**3,481**	**14.2**	**21**	**1.0**	**99**
18.30	21.90			Limonite							
21.90	25.50			Dolomite breccia	**3**	**388**	**311**	**5.5**	**93**	**0.2**	**204**
25.50	29.00			Limonite							
29.00	35.70	Anisian	Mineralized zone	Dolomite breccia	1	422	21	3.7	55	0.3	189
35.70	47.80				**12**	**55**	**8,610**	**8.0**	**49**	**2.5**	**113**
47.80	54.00			Siltstone breccia	*19*	*32*	*283*	*4.2*	*2,668*	*3.1*	*14,002*
54.00	75.50			Dolomite breccia	**3**	**99**	**3,841**	**8.3**	**29**	**2.0**	**68**
75.50	80.00	Lower Triassic		Shale breccia	0	81	41	3.1	80	1.1	114
80.00	87.00			Siltstone breccia							
87.00	102.50				**1**	**128**	**417**	**7.7**	**113**	**0.7**	**185**
102.50	112.50			Limestone breccia							
112.50	130.90			Sandstone breccia	0	102	1	1.7	1	0	3

From the 23 boreholes of the latest exploration program (with varying lengths to max. 200 m), the copper-enriched intervals (>0.2% Cu, min. 2 m apparent thickness) have shown the following main parameters:

Number of intervals	Average length (m)	Ag (ppm)	Cu (%)	Ba (ppm)	Fe (%)	Pb (%)	S (%)	Zn (%)
35	5.0	6.6	0.45	135	16.3	0.07	2.2	0.14

The element concentrations indicate the presence of silver in the copper ores (possibly related to tetrahedrite), high Fe grades indicating the iron-enriched carbonate as frequent host lithology, low sulfide content in general and the absence of Pb and Zn enrichments.

Our observations support that copper sulfides are bound to carbonate rocks affected by metasomatism, but enrichments can occur inside the bodies as well as at the edges. The grade of the copper enrichment does not depend on the grade of the sideritization, and it also occurs in the marginal parts of the mining area. At the border of the metasomatized complex, it was found in brecciated carbonate rocks of fault zones. In a single case, the T-17 borehole crosscut a fault zone in underlying sandstone beds with a quartz–ankerite vein containing chalcopyrite and 0.1–0.2 wt% assayed copper enrichment. Sandstone bodies of the oxidized zone, however, may have higher Cu grades hosted by secondary minerals (e.g., native copper, malachite, azurite, and chalcocite).

Ore microscopy and electron microprobe observations and measurements

The most frequently occurring opaque minerals in the samples containing copper sulfide mineralization are pyrite (FeS_2), chalcopyrite ($CuFeS_2$), bornite (Cu_5FeS_4), tetrahedrite ($Cu_6[Cu_4(Fe,Zn,Hg,Ag)_2]Sb_4S_{13}$), tennantite ($Cu_6[Cu_4(Fe,Zn,Hg,Ag)_2]As_4S_{13}$), chalcocite ($Cu_2S$), digenite ($Cu_9S_5$), and covellite (CuS). Further accessory sulfides are marcasite (FeS_2), galena (PbS), sphalerite (ZnS), famatinite (Cu_3SbS_4), enargite (Cu_3AsS_4), and mawsonite ($Cu_6Fe_2SnS_8$). The sulfides occur in veins, vugs, and pores of the carbonate host rock, and in the matrix of brecciated carbonates as well (Fig. 3a), in several cases with barite ($BaSO_4$) and sparry carbonates. These minerals also often occur in overprinting veins and crosscutting the sulfide-bearing matrix (Fig. 3b). Ca–Mg–Fe carbonate minerals of the host rock show variable composition (calcite–dolomite–magnesite and dolomite–ankerite–siderite series) zoning that is common with changing metal content within a single grain. Quartz occurs as pore filling inside the clasts of the breccia, or as single clasts overgrown by sulfides and barite. Further minerals filling the interspaces of the ore minerals or of the host rock are cassiterite (SnO_2), spherical, zoned rosasite and Zn–rosasite [$(Cu,Zn)_2(CO_3)(OH)_2$–$(Zn,Cu)_2(CO_3)(OH)_2$], malachite [$Cu_2(CO_3)(OH)_2$], crust-forming iron-hydroxides, other Cu- and Pb-oxides, Cu-sulfates and Cu–U-sulfates.

Pyrite occurs in several forms. The prevalent grain shape is hypidiomorphic, often fractured, sometimes altered to marcasite. Chalcopyrite, bornite, and fahlore commonly occur in the fractures and around the grains. Bornite and barite can also be found as enclosures in hypidiomorphic pyrite; the bornite is always partly altered to chalcocite and/or digenite. Another typical form of the pyrite is the concentric crystal aggregate, usually bound to covellite, which was formed after chalcopyrite (Fig. 2a). In some samples, tennantite is radially intergrown with pyrite, or these minerals are changing in concentric zones, sometimes overgrown by chalcopyrite altered to covellite (Fig. 3c). Beyond these forms, pyrite can also be collomorph, in some cases, surrounding hypidiomorphic aggregates. The intergrowth of this pyrite with tennantite or sometimes with covellite also can be observed; in the outer tennantite zones, barite also occasionally appears. Finally, pyrite can occur framboidally or as disseminated hypidiomorphic grains of ~10 μm diameter. Chalcopyrite sometimes can also occur among the microcrystals. However, this form is not bound to the copper sulfides, and the dissemination is present everywhere in the host rock. Microprobe analyses of certain pyrite grains or aggregates have shown As (1–3 wt%) and Cu (1–8 wt%) enriched zones; in one sample also Pb enrichment (Fig. 3d).

Bornite and **chalcopyrite** nearly always fill together the interspaces of the idiomorphic and hypidiomorphic carbonate and pyrite grains (Figs 2b and 3e). Chalcopyrite grew around or in the fractures of the bornite aggregates. At the contact of the minerals, flame structure of the chalcopyrite within the bornite is typical in several cases (Fig. 3f). Thin chalcopyrite lamellae often follow the cleavage of the bornite (Fig. 2c), becoming more frequent toward the edge; in some cases, the edge consists entirely of chalcopyrite. At the grain boundaries and the fractures filled with chalcopyrite, covellite alteration is characteristic (Fig. 2d); in bornite, it can also occur within the aggregates. In some cases, digenite and pyrite can also be found among the covellite crystals (Fig. 2e). Mawsonite occurs as inclusion in bornite (Fig. 3g).

Fahlore (**tennantite** and **tetrahedrite**) occurs in three forms in the texture, and differences in the chemical composition of these forms can also be measured. Grains of the **first group** occur either as inclusions in pyrite, chalcopyrite, and bornite (Fig. 3h) or grown on pyrite, overgrown and substituted by bornite and chalcopyrite (Fig. 2f and g). Tetrahedrite always occurs at the edge or in the fractures of tennantite. Some fahlore grains are neither tennantite nor tetrahedrite by composition, probably having a mixed transitional structure. Energy Dispersive Spectrum (EDS) measurements of these grains show the presence of Fe, Zn, Cu, and often of mercury (2 wt% on avg., 8 wt% max.) and of silver (2 wt% on avg., 8 wt% max.). Tennantite usually contains more iron (5.22 wt% on avg.) than zinc (1.56 wt% on avg.), but fahlore with mixed structure and tetrahedrite contains these in nearly equal quantities (3.25 wt% Fe and 2.81 wt% Zn on avg.).

The **second group** also comprises tennantite, tetrahedrite, and fahlore of mixed structure. These occur in veins within chalcopyrite (Fig. 2h), or as overgrowth and substituting grains on chalcopyrite. Chalcopyrite altered to covellite at the edges can also be overgrown by this fahlore (Fig. 3i); covellite, however, can also be the

alteration product of fahlore in other cases (Fig. 2i). The fahlore can be zoned with tetrahedrite or mixed structure core and alternating tennantite and tetrahedrite layers, usually ending with an outer tetrahedrite layer. In some cases, a thin tennantite crust surrounds the tetrahedrite or mixed structure grains. Zinc content (5.02 wt% on avg.) of the fahlore grains of this group exceeds the iron content (2.05 wt% on avg.) and these also contain Hg and Ag like the first group.

Fahlore of the **third group** should be described rather as **zinc-tetrahedrite** ($Cu_{10}Zn_2Sb_4S_{13}$), although it can also contain minor Fe (max. 1 wt%) and As (max. 4.6 wt%). Sometimes Hg (max. 1.8 wt%) and Pb (max. 4.6 wt%) could also be measured. This mineral occurs in veins within chalcopyrite, grown on altered chalcopyrite and also grown on fahlore of the first and the second groups. In one case, it was found in a vein within chalcopyrite comprised of famatinite and enargite (Figs 2j and 3j). Famatinite at the vein walls is intergrown with enargite inside, and at the center of the vein, there is the Zn-tetrahedrite, substituting the previous minerals.

Some samples contained accessory **galena** and **sphalerite**. Xenomorphic galena grains typically have a diameter of 1–5 μm, and these occur as inclusions in pyrite, as overgrowths on pyrite, or overgrown by chalcopyrite and tetrahedrite (Figs 2k and 3k). Assays of galena crystals contain 1–1.5 wt% Sr, and in one case ~20 wt% Ag (without Sr in this case). Sphalerite fills the interspaces of chalcopyrite and fahlore. Sometimes it is a dominant constituent overgrowing every other mineral, including remnants of chalcopyrite, covellite, and fahlore grains (Fig. 2l); marcasite may also join to the assemblage. Sphalerite occurs in several cases at grain boundaries of chalcopyrite altered to covellite together with Zn-tetrahedrite, but also surrounding Zn-tetrahedrite. In such case, it also substitutes the Zn-zoned rosasite filling a void rimmed by Zn-tetrahedrite (Fig. 3l).

Barite is a common mineral of the sulfide-dominated mineral assemblage, occurring also in several forms in the texture. It can occur as inclusion of pyrite, bornite, and tennantite from the first group; substituting pyrite and overgrown by bornite, as overgrowth on chalcopyrite altered to covellite and digenite or as overgrowth on fahlore substituted by Zn-tetrahedrite. Barite also occurs in the famatinite–enargite–Zn-tetrahedrite vein and as a vein-filling, crosscutting pyrite–chalcopyrite–fahlore assemblage.

Interpretation of the observations

The paragenetic sequence derived from the observations is summarized in Fig. 4. Overprinting relationships described by Koch et al. (1950) were mostly supported by our observations, but the number of possibilities was increased, as several minerals have more than one generation, so new sequences could be identified.

Copper sulfides and associated minerals overgrow the carbonate grains of the host rock, which occur in veins and in the cement of brecciated rocks. The oldest detected phases are found as inclusions of hypidiomorphic pyrite, represented by

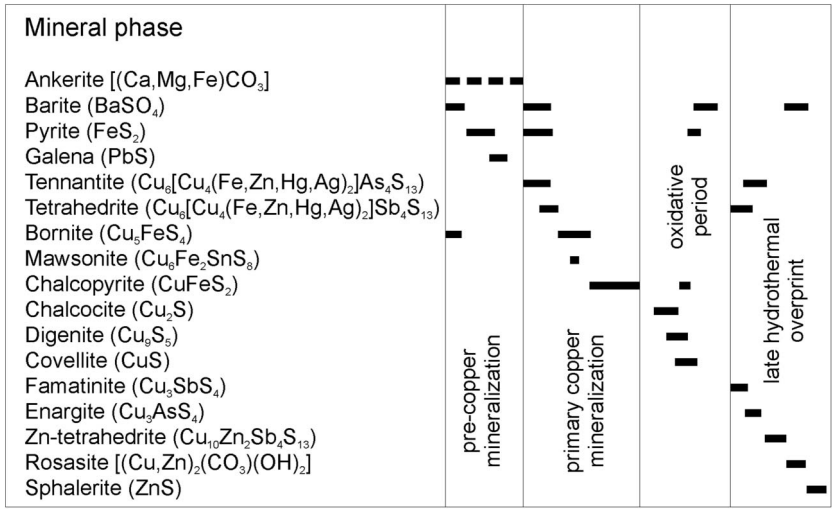

Fig. 4
Evolution chart of the described mineral assemblage related to the copper sulfide mineralization

bornite and barite. The first significant copper mineralization (primary copper mineralization) followed the precipitation of this pyrite and sparry carbonates of dolomite–ankerite composition, also overprinting the products of iron metasomatism described by Pantó (1956). Ore controls were similar in all of these mineralization events: fault zones and fractured, brecciated rocks, mainly carbonates. Mineralized host carbonate rocks may previously have been only weakly metasomatized, but Fe-containing, zonal carbonate minerals are always present, even in sandstone hosted occurrences.

Mineralization began with the crystallization of tennantite and pyrite forming spherical assemblages, occasionally also containing copper and barite. Tennantite and pyrite are sometimes intergrown zonally. During the ongoing crystallization, the composition of the fahlore of the first group changed gradually from tennantite to tetrahedrite with transitional structures, and pyrite formation ceased. After that, bornite formed in major quantity and substituted partly in the previously precipitated minerals. According to Pósfai (1989), who measured the appearance of bornite polymorphs within the assemblage, bornite included in pyrite had a formation temperature over 228 °C; other bornite crystals associated with chalcopyrite were formed at approximately 170 °C; the latter temperature may characterize this phase of the mineralization.

In the following stage, chalcopyrite was formed as a substituent of bornite, fahlore, and pyrite, and also as new grains, thus becoming the most frequently occurring copper mineral of the assemblage. Bornite was substituted by the chalcopyrite along preferred crystallographic orientations, with characteristic flame structures. The

crystallization of chalcopyrite and alteration of previous copper minerals indicates an increasing sulfur fugacity and iron content of the system.

After chalcopyrite crystallization, the environment became oxidative in certain parts of the deposit, because the oxidation of bornite has led to the digenite–covellite–chalcopyrite association; then, chalcopyrite was altered to covellite and pyrite. Copper carbonates and other oxidation products may have been formed as well. These can be separated from the recent subsurface oxidation zone minerals by a subsequent hydrothermal overprint, which is not bound to the primary copper mineralization but overlaps with it in several places.

This overprint is the mineralization of barite, quartz, and the mineral assemblage described as late hydrothermal mineralization by Szakáll (2001). As we have only studied samples of such overlapping sites here, the description does not cover the total variability of all possible types of parageneses, only the one developed in primary copper sulfide ores. The first phase of this mineralization is fahlore of the second group, occurring in veins and fractures of chalcopyrite. The core of the grains is tetrahedrite; thereafter, the composition shifted toward tennantite of mixed structure, and occasionally zoned with transitional members. The observed famatinite and enargite vein was probably formed parallel to this, as an increasing As/Sb ratio leads to the zoned growth of these minerals as well. In the course of the ongoing crystallization, both mineral groups are partly substituted by Zn-tetrahedrite, with some arsenic content at the start. The latest phases of the mineralization process are also barite and sphalerite, which also substitute copper sulfides and copper carbonates.

No ore samples have been found with the coexisting carbonate-hosted zinc–lead sulfide and primary copper sulfide mineralization, so the order of their evolution remains ambiguous. Accessory galena grains of the copper ore cannot be exactly placed in the paragenetic sequence due to their small grain size and a few observed textural relationships, but probably these are older than the primary copper mineralization and younger than the hypidiomorphic pyrite. Major occurrences of Zn-bearing minerals in copper ore and Cu-bearing minerals in zinc–lead ore all proved to be late hydrothermal or oxidative overprints along fractures and grain edges.

Geochemical evidence of the spatial separation of Zn–Pb and Cu ores and also the general occurrence of fahlore along with bornite and chalcopyrite is provided by the correlation of Cu with Sb, As, and Bi (Tables 2 and 3) in the assayed sections of T-11, 11A, 11B, 12, 12A, 14, 15, and 15A exploration boreholes (314 assayed samples). Pb, Ag, Zn, and Cd form another strongly correlated group. However, according to the Sb/Cu and the (Sb + As)/Cu ratios, a maximum of 5%–10% of the total copper content can be hosted by tetrahedrite and tennantite. If the galena-bearing (Zn–Pb ore) sections are excluded from the sample (258 elements remaining), Ag and Hg are well correlated with Cu. These elements are enriched in galena, but fahlores also incorporate both of these in minor quantity, reaching a concentration <100 ppm in the assay only.

Table 2
Linear correlation coefficients of the chemical elements conjugated with the base metal mineralization from the assayed sections of boreholes T-11, 11A, 11B, 12, 12A, 14, 15, and 15A (letters denote holes started from the same numbered point with different inclinations). Number of sample elements: 314; elements with Cu content >0.1 wt%: 116 (37%); elements with Cu content >0.5 wt%: 32 (10.2%); median Cu: 275 ppm; max. Cu: 2.44 wt%

	Ag	As	Bi	Ca	Cd	Cu	Fe	Hg	Mg	Pb	S	Sb	Zn
Ag	***1.00***												
As	0.45	***1.00***											
Bi	0.13	0.37	***1.00***										
Ca	–0.06	0.14	0.16	***1.00***									
Cd	***0.82***	0.27	–0.06	–0.15	***1.00***								
Cu	0.21	**0.51**	**0.68**	0.25	–0.01	***1.00***							
Fe	0.03	0.08	0.35	–0.38	–0.07	0.26	***1.00***						
Hg	0.25	0.19	–0.02	–0.08	0.38	–0.02	–0.08	***1.00***					
Mg	–0.11	0.18	0.29	**0.53**	–0.18	0.33	0.12	–0.10	***1.00***				
Pb	***0.85***	0.28	–0.06	–0.15	***0.86***	–0.04	–0.06	0.43	–0.18	***1.00***			
S	**0.70**	**0.52**	0.18	–0.08	**0.61**	0.15	0.02	0.34	0.03	**0.59**	***1.00***		
Sb	0.34	**0.65**	0.42	0.28	0.18	***0.71***	0.11	0.10	0.33	0.14	0.34	***1.00***	
Zn	***0.81***	0.27	–0.06	–0.16	***0.97***	–0.03	–0.08	**0.51**	–0.19	***0.88***	**0.61**	0.15	***1.00***

Coefficient values are bold characters if exceeding 0.5 and italic characters if exceeding 0.7

Possible geologic and genetic relationships of the copper sulfide mineralization

When comparing the Rudabánya primary copper sulfide deposit with other similar deposits in the metallogenic zone, we must separate the features of the copper mineralization from those of the earlier and later ore-forming processes, which are also present in the Rudabánya ore-bearing complex. For example, the Kremikovci siderite–barite–sulfide deposit (Damyanov 1996) has many similarities with the corresponding Rudabánya mineralization and with some of its overprints. The Lower Triassic sedimentary exhalative iron ore formation of Kremikovci and its late diagenetic redeposition may be considered as analogous events to the sedimentary iron accumulation and late diagenetic remobilization of similar age at Rudabánya (Bodor et al. 2016). Kremikovci also has subsequent sulfide mineralization (mainly Pb, Zn, less Cu) and an extended supergene limonite zone. However, a copper sulfide mineralization analogous with the one in Rudabánya is not known at Kremikovci.

Table 3
Linear correlation coefficients of the chemical elements conjugated with the base metal mineralization from a sample of previous assays with Pb and Zn <0.1 wt% only. Number of sample elements: 258; elements with Cu content >0.1 wt%: 96 (37.2%); elements with Cu content >0.5 wt%: 27 (10.5%); median Cu: 274.5 ppm; max. Cu: 1.57 wt%

	Ag	As	Bi	Ca	Cd	Cu	Fe	Hg	Mg	Pb	S	Sb	Zn
Ag	***1.00***												
As	0.41	***1.00***											
Bi	**0.54**	0.39	***1.00***										
Ca	0.28	0.26	0.19	***1.00***									
Cd	0.15	0.38	0.05	0.03	***1.00***								
Cu	**0.62**	0.48	**0.69**	0.27	0.02	***1.00***							
Fe	0.07	0.03	0.27	–0.43	–0.03	0.19	***1.00***						
Hg	0.46	**0.57**	0.39	0.18	0.20	**0.56**	0.12	***1.00***					
Mg	0.27	0.38	0.37	0.50	0.04	0.42	0.10	0.29	***1.00***				
Pb	0.30	0.36	0.16	0.10	**0.65**	0.04	–0.08	0.20	0.05	***1.00***			
S	0.37	**0.54**	0.42	0.10	0.19	0.36	0.01	0.36	0.27	0.42	***1.00***		
Sb	0.48	**0.67**	0.45	0.32	0.13	***0.73***	0.06	***0.75***	0.43	0.06	0.38	***1.00***	
Zn	0.23	0.36	0.19	0.18	***0.81***	0.11	–0.02	0.21	0.20	**0.67**	0.20	0.13	***1.00***

Coefficient values are bold characters if exceeding 0.5 and italic characters if exceeding 0.7

McKinstry (1963) set the first detailed summary of field and laboratory observations related to Cu–Fe–As–S systems, and pointed out that the most common evolution is a trend with continuous enrichment of sulfur at a relatively constant Cu:Fe ratio. In the interpretation of this trend, he concluded that sulfur enrichment occurs spatially downward and inward, and is temporally a late-stage progression of the hydrothermal system.

Cox and Bernstein (1992) have summarized dolomite-hosted metasomatic base metal mineralization systems with Cu–Fe–As–S mineralization as a part of the Kipushi-type Cu–Pb–Zn deposits. Most of these deposits are related to fault zones, and underlying evaporite beds are often present as possible sources of sulfur. In this deposit model group, Tsumeb (Namibia) has been studied in detail for the evolution of its Cu–As–S mineral assemblage (Haynes 1985), with very similar mineral paragenesis (chalcopyrite, bornite, chalcocite, tennantite, and enargite) as in Rudabánya. The observed paragenetic relationships of copper minerals are consistent with a model of upward and outward moving chemical fronts. The paragenetic sequence related to the

Cu phases can have been produced from a single acidic, Cu-rich fluid with an initial temperature over 250 °C, simply by passing the fluid through chemically receptive dolomites over a period of time. The reaction with dolomite, increasing pH values of the solution, shifts the activities of the solved components onto a path where the first stable mineral phases are sulfosalts (tennantite and enargite), then bornite and chalcocite, and finally chalcopyrite before reaching equilibrium with the dolomite host. So far, this corresponds to the situation observed in Rudabánya; at Tsumeb, however, continuing acidic fluid input resulted in a reverse alteration sequence in the outer zones.

In a regional context, the Rudabánya deposit belongs to the cluster of vein-type siderite–Cu mineralizations in the synthesis of geology of major modern Alpine–Carpathian ore deposits (Neubauer 2002). These deposits were mostly interpreted as being remobilized during Cretaceous metamorphism without genetic link to any known igneous source. The closest important metallogenic zone with a similar style of copper mineralization is the Gemerids of the Slovak Ore Mountains. The Paleozoic host rocks of this zone also form the original basement of the Silicikum including the Rudabánya ore-bearing complex. With regard to vein-type siderite–copper deposits, Grecula et al. (1995) stressed the importance of metamorphism and tectonism in the formation of ore-bearing fluids, modeling a "tectonic hydrothermal pump" which is activated in several stages and has mobilized various ore-forming elements from Paleozoic host rocks. They also described the copper vein mineralizations as hosted by the transpressive structures and shear zone of the Alpine movements, with ankerite, quartz, chalcopyrite, and tennantite mineral assemblage. The time range was estimated as 70–110 ± 10 Ma, i.e., Upper Cretaceous to Paleocene. Radvanec et al. (2004) have provided further ample evidence of this metamorphogenic model, by placing the peak intensity of the siderite–barite–sulfide metasomatism in the period of uplift of the Variscan metamorphic complex during the Alpine orogenic processes. It was stressed that the genetic interpretation of the siderite–sulfide–barite mineralization is far from complete, although the previously assumed role of hypothetic deep-seated Cretaceous–Tertiary magmatic source was excluded. Bodor et al. (2013b) have provided mineralogical evidence of the alterations caused by deep burial diagenesis or early metamorphism in the ore-bearing rocks at Rudabánya. These data underline the similarity of Rudabánya and several copper deposits of the Gemerids of the Slovak Ore Mountains, which were explained using the metamorphogenic model.

Along the Darnó Zone, the relationship of the Rudabánya and Recsk porphyry and skarn copper mineralizations was investigated by Baksa (1986). He did not find any common points in their genesis. In the light of later borehole results, we assume that the spatial link of these mineralizations with Late Paleozoic evaporites and Triassic–Jurassic copper-bearing basalt within the Darnó Zone allows outlining a probable model where copper is sourced from the basalt and sulfur from the evaporites, while the mobilizing events are related to structural movements in the Darnó Zone regional fault system (Földessy et al. 2012b).

Conclusions

The primary copper mineralization of Rudabánya is a separate stage within the sequence of ore-forming processes, overprinting the siderite metasomatism and probably not connected with any lead and zinc mineralizations. Host rocks are carbonates affected by the previous iron metasomatism, but copper mineralization is not correlated with its grade or zones. Ore controls are breccia zones; copper sulfides were precipitated in the matrix of the carbonate clasts. Ore bodies (using 0.2% Cu cut-off grade) are either isometric or tabular blocks of some ten meters in size. Several adjacent ore bodies form dense clusters. The copper-mineralized region thus extends over 1 km, with a width of 200–300 m. The mineralization began with crystallization of fahlore continued with bornite, and the final mineral phase was chalcopyrite replacing the previous ones. Oxidation and late-stage hydrothermal mineralization remobilized the base metals from the altered minerals of this and previous mineralizations, producing polymetallic supergene enrichments.

References

Baksa, Cs. 1986: A recski és a rudabányai ércesedések eredetének összehasonlító elemzése (A comparative analysis of the origin of the ore mineralizations of Recsk and Rudabánya). – Földtani Közlöny, 116, pp. 353–361. (in Hungarian)

Balla, L. (Ed) 1987: Rudabányai vasércbányászat. Bányabezárási dokumentáció (Iron ore mining at Rudabánya. Mine closure documentation). – Manuscript, Heavy Industrial Technical University, Miskolc, 441 p. (in Hungarian)

Bodor, S., F. Kristály, N. Németh, A. Gerges, A. Kasó Jr. 2013a: A savanyú pátvasérc ásványtani és geokémiai jellegei a rudabányai ércelőfordulásban (Mineralogical and geochemical characteristics of the 'acidic spar ore' in the Rudabánya ore deposit). – Bányászati és Kohászati Lapok, Bányászat, 146/5–6, pp. 33–38. (in Hungarian)

Bodor, S., J. Földessy, F. Kristály, N. Zajzon 2013b: Diagenesis and ore forming processes in the Bódvaszilas Sandstone of the Rudabánya ore deposit, NE Hungary. – Carpathian Journal of Earth and Environmental Sciences, 8/4, pp. 147–153.

Bodor, S., M. Polgári, I. Szentpétery, J. Földessy 2016: Microbially mediated iron ore formation, Silicic Superunit, Rudabánya, Hungary. – Ore Geology Reviews, 72, pp. 391–401.

Cox, D.P., L.R. Bernstein 1992: Descriptive model of Kipushi Cu–Pb–Zn. Model 32c. – In: Cox, D.P., D.A. Singer (Eds): Mineral Deposit Models, USGS Bulletin, 1693, 227 p.

Csalagovits, I. 1973: A Rudabánya környéki triász összlet geokémiai és ércgenetikai vizsgálatának eredményei (Results of geochemical and ore genetical investigations of a Triassic sequence in the vicinity of Rudabánya). – Annual report of the Hungarian Geological Institute, 1971, pp. 61–90. (in Hungarian)

Damyanov, Z.K. 1996: Ore petrology, whole-rock chemistry, and zoning of the Kremikovci carbonate-hosted sedimentary exhalative (+Mn)–barite–sulfide deposit, Western Balkan, Bulgaria. – Neues Jahrbuch für Mineralogie, 174, pp. 1–42.

Fodor, L., L. Csontos, G. Bada, I. Györfi, L. Benkovics 1999: Tertiary tectonic evolution of the Pannonian basin system and neighbouring orogens: a new synthesis of paleostress data. – In: Durand, B., L. Jolivet, F. Horváth, M. Séranne (Eds): The Mediterranean Basins: Tertiary Extension within the Alpine Orogen, Geological Society, Special Publications, London, UK, 156, pp. 295–334.

Földessy, J., N. Németh, A. Gerges 2010: A rudabányai színesfém-ércesedés újrakutatásának előzetes földtani eredményei (Preliminary results of the re-exploration of the Rudabánya base metal ore deposit). – Földtani Közlöny, 140/3, pp. 281–292. (in Hungarian)

Földessy, J., N. Németh, L. Kupi, A. Gerges, A. Kasó Jr., Sz. Tóth 2012a: Rudabánya – egy jelentős színesfémérc-lelőhely születése felé (Rudabánya – Towards the birth of a significant base metal ore occurrence). – Bányászati és Kohászati Lapok, Bányászat, 145/5, pp. 7–12. (in Hungarian)

Földessy, J., N. Németh, G. Szebényi, É. Hartai 2012b: Copper ore mineralizations along the Darnó shear zone, Hungary – Similarities and differences. – Second International Copper Mining Conference, Lubin, Poland, Conference Abstracts, pp. 70–75.

Földessy, J., N. Németh, A. Gerges, S. Bodor, A. Kasó Jr. 2014: Az arany geokémiai eloszlása a rudabányai ércelőfordulás földtani környezetében (Geochemical distribution of gold in the Rudabánya Ore Bearing Complex). – In: Fehér, B. (Ed): The lure of minerals: Anniversary volume in the honor of Sándor Szakáll's 60th birthday, Herman Ottó Múzeum és Magyar Minerofil Társaság, Miskolc, Hungary, pp. 75–83. (in Hungarian)

Grecula, P., A. Abonyi, M. Abonyiová, J. Antaš, B. Bartalský, J. Bartalský, I. Dianiška, R. Ďud'a, M. Gargulák, L'. Gazdačko, J. Hudáček, J. Kobulský, L. Lörincz, J. Macko, D. Návesňák, Z. Németh, L. Novotný, M. Radvanec, I. Rojkovič, L. Rozložník, C. Varček, Z. Zlocha 1995: Mineral Deposits of the Slovak Ore Mountains. – Geokomplex, Bratislava, Slovakia, 1, 833 p.

Haynes, F. 1985: A geochemical model for sulfide paragenesis and zoning in the Cu–Fe–As–S system (Tsumeb, South West Africa/Namibia). – Chemical Geology, 47, pp. 183–190.

Koch, S., Gy. Grasselly, É. Donáth 1950: Magyarországi vasércelőfordulások ásványai (Minerals of Hungarian iron ore deposits). – Acta Mineralogica Petrographica, 4, pp. 1–41. (in Hungarian)

Korpás, L., A.H. Hofstra, L. Ódor, I. Horváth, J. Haas, T. Zelenka 1999: Evaluation of the prospected areas and formations. – Geologica Hungarica series Geologica, 24, pp. 197–294.

Kovács, S., Gy. Less, O. Piros, Zs. Réti, L. Róth 1989: Triassic formations of the Aggtelek–Rudabánya Mountains (NE Hungary). – Acta Geologica Hungarica, 32/1–2, pp. 31–63.

Kristály, F., S. Szakáll, N. Németh, N. Zajzon 2010: A smithsonit különböző szövet-szerkezeti típusai a rudabányai karbonátos érctelepben (Texture types of the smithsonite in the Rudabánya carbonate ore deposit). – A Miskolci Egyetem Közleménye, A, Bányászat, 79, pp. 27–38. (in Hungarian)

Kupi, L. 2011: Paragenetikai vizsgálatok a rudabányai színesfémércesedésben transzparens- és opakoptikai megfigyelések alapján (Paragenetic studies in the Rudabánya base metal mineralization based on transparent and opaque optical observations). – Manuscript, Research report on the study at the University of Oviedo, 22 p. (in Hungarian)

McKinstry, H. 1963: Mineral assemblages in sulfide ores: The system Cu–Fe–As–S. – Economic Geology, 53, pp. 483–505.

Nagy, B. 1982: A rudabányai ércesedés összehasonlító ércgenetikai vizsgálata (A comparative metallogenetic study of the Rudabánya mineralization, N Hungary). – Annual report of the Hungarian Geological Institute, 1980, pp. 45–58. (in Hungarian)

Németh, N., A. Kasó Jr. 2014: Talajgeokémiai vizsgálatok a rudabányai színesfémérc-előfordulás kutatásában (Soil geochemistry studies in the exploration of the Rudabánya base metal deposit). – In: Fehér, B. (Ed): The lure of minerals: Anniversary volume in the honor of Sándor Szakáll's 60th birthday. Herman Ottó Múzeum és Magyar Minerofil Társaság, Miskolc, Hungary, pp. 191–202. (in Hungarian)

Németh, N., J. Földessy, L. Kupi, J.G. Iglesias 2013: Zn–Pb mineralization types in the Rudabánya ore bearing complex. – Carpathian Journal of Earth and Environmental Sciences, 8/1, pp. 47–58.

Neubauer, F. 2002: Contrasting late cretaceous with the neogene ore provinces in the Alpine–Balkan–Carpathian–Dinaride collision belt. – In: Blundell, D.J., F. Neubauer, A. von Quadt (Eds): The Timing and Location of Major Ore Deposits in an Evolving Orogen. Geological Society of London, Special Publication, 204, pp. 81–103.

Pantó, G. 1956: A rudabányai vasércvonulat földtani felépítése (Geology of the Rudabánya ore bearing complex). – Annals of the Hungarian Geological Institute, 44/2, pp. 329–637. (in Hungarian)

Pantó, E., G. Pantó, T. Podányi, K. Moser (Eds) 1957: Rudabánya ércbányászata (Ore Mining of Rudabánya). – Hungarian Mining and Metallurgical Society, Budapest, Hungary, 421 p. (in Hungarian)

Pósfai, M. 1989: Bornite from Rudabánya: An electron diffraction study. – Acta Geologica Hungarica, 32/1–2, pp. 231–240.

Radvanec, M., P. Grecula, K. Žák 2004: Siderite mineralization of the Gemericum superunit (Western Carpathians, Slovakia): Review and a revised genetic model. – Ore Geology Reviews, 24, pp. 267–298.

Szakáll, S. 2001: Rudabánya ásványai (Minerals of Rudabánya). – Kőország Kiadó, Budapest, Hungary, 176 p. (in Hungarian)

Szalay, I., L. Verő, A. Zsille 1974: Geofizikai kutatás a Darnó-vonal ércesedett tektonikai övezetében (Geophysical survey in the ore bearing tectonic belt of the Darnó Line). – Annual report of the Eötvös Loránd Geophysical Institute, 1973, pp. 28–31. (in Hungarian)

Szentpétery, I., Gy. Less (Eds) 2006: Az Aggtelek–Rudabányai hegység földtana. Magyarázó az Aggtelek–Rudabányai-hegység 1988-ban megjelent 1:25000 méretarányú fedetlen földtani térképéhez (Geology of the Aggtelek–Rudabánya Mts. Explanations to the 1:25000 Scale Geological Map of the Aggtelek–Rudabánya Mts. Published in 1988). – Hungarian Geological Institute, Budapest, Hungary, 92 p. (in Hungarian)

Zelenka, T., Cs. Baksa, Z. Balla, J. Földessy, K. Járányi-Földessy 1983: Mezozoos ősföldrajzi határ-e a Darnó vonal? (Is the Darnó Lineament a Mezozoic paleogeographic border?). – Földtani Közlöny, 113/1, pp. 27–37. (in Hungarian)